



Morphometric Analysis of Greater Palatine Canal by Computed Tomography

Canalis Palatinus Major Morfometrisinin Bilgisayarlı Tomografi ile Değerlendirilmesi


Hilal GÜZEL¹

 0000-0001-7692-8890


Ozan TURAMANLAR²

 0000-0002-0785-483X


Esra KOYUNCU³

 0000-0003-3330-0096

Erdal HORATA⁴

 0000-0003-1359-228X

Çiğdem ÖZER GÖKASLAN⁵

 0000-0001-5345-1735

¹PhD in Anatomy, Free Scholar,
Hamminkeln, Germany

²Department of Anatomy, Katip Çelebi
University Faculty of Medicine, İzmir,
Türkiye

³Department of Anatomy,
Afyonkarahisar Health Sciences
University Faculty of Medicine,
Afyonkarahisar, Türkiye

⁴Department of Orthopedic Prosthetic-
Orthosis, Afyonkarahisar Health
Sciences University Health Services
Vocational School, Afyonkarahisar,
Türkiye

⁵Department of Radiology,
Afyonkarahisar Health Sciences
University Faculty of Medicine,
Afyonkarahisar, Türkiye

Corresponding Author

Sorumlu Yazar

Erdal HORATA
erdalhorata@gmail.com

Received / Geliş Tarihi : 10.10.2023

Accepted / Kabul Tarihi : 17.12.2023

Available Online /

Çevrimiçi Yayın Tarihi : 22.12.2023

ABSTRACT

Aim: The greater palatine canal connects to the oral cavity through the greater palatine foramen. Preoperatively identifying the morphology of the greater palatine canal and greater palatine foramen is very important to avoid possible complications during surgery. This study aimed to evaluate the greater palatine canal and surrounding anatomical structures using computed tomography.

Material and Methods: Images from 100 patients (35 female and 65 male) who had previously undergone computed tomography for various reasons were evaluated. The study data were divided into three age groups, <20 years, 20-60 years, and >60 years. Morphological parameters measured in this study included; diameter measurement from the widest part of the canal, length of the canal, beginning diameter of the canal, the ends diameter of the canal, localization of the canal entrance with respect to the third molar tooth, distance of the canal entrance to palatine suture. The values obtained from the measurements were compared in terms of age group, gender, and side.

Results: The mean length of the canalis palatinus major was 15.19±4.38 mm. The diameter of the widest part of the canal and the end of the canal, and the distance between the canal entrance and the sutura palatina increased with age, but these increases were not statistically significant.

Conclusion: Proper administration of anesthesia through the greater palatine foramen in maxillofacial surgeries and related applications requires a detailed understanding of the anatomy of the greater palatine canal, and the results of the present study will contribute to the understanding of this anatomy.

Keywords: Greater palatine canal; anatomy; computed tomography.

ÖZ

Amaç: Canalis palatinus major, foramen palatinum majus aracılığı ile ağız boşluğuna bağlanır. Canalis palatinus major ve foramen palatinum majus morfolojisinin ameliyat öncesinde belirlenmesi, ameliyat sırasında ortaya çıkabilecek olan olası komplikasyonlardan kaçınmak için oldukça önemlidir. Bu çalışmanın amacı, canalis palatinus major ve çevresindeki anatomik yapıların bilgisayarlı tomografi ile değerlendirilmesidir.

Gereç ve Yöntemler: Daha önce çeşitli nedenler ile bilgisayarlı tomografisi çekilmiş olan 100 hastanın (35 kadın ve 65 erkek) görüntüleri incelendi. Çalışma verileri <20 yaş, 20-60 yaş ve >60 yaş olmak üzere üç yaş grubuna ayrıldı. Bu çalışmada ölçülen morfolojik parametreler; kanalın en geniş kısmından çap ölçümü, kanalın uzunluğu, kanalın başlangıç çapı, kanalın uç çapı, kanal girişinin üçüncü molar dişe göre lokalizasyonu ve kanal girişinin sutura palatinaya olan uzaklığıdır. Ölçümler sonucu elde edilen değerler, yaş grubu, cinsiyet ve taraf açısından birbiriyle karşılaştırıldı.

Bulgular: Canalis palatinus majorun ortalama uzunluğu 15,19±4,38 mm idi. Kanalın en geniş yerinin çapı ile bitiş yerinin çapı ve kanal girişi ile sutura palatina arasındaki mesafe, yaş ile birlikte artmış olmakla birlikte bu artışlar istatistiksel olarak anlamlı değildi.

Sonuç: Maksillofasiyal cerrahilerde ve bununla ilgili olan uygulamalarda anestezinin foramen palatinum majus yolu ile uygun bir şekilde uygulanması için canalis palatinus major anatomisinin ayrıntılı bir şekilde anlaşılması gerekmektedir ve bu çalışmanın sonuçları bu anatominin anlaşılmasına katkı sunacaktır.

Anahtar kelimeler: Canalis palatinus major; anatomi; bilgisayarlı tomografi.

INTRODUCTION

The greater palatine canal (GPC) is mostly placed opposite the third molar. It connects with the oral cavity via the greater palatine foramen (GPF) (1). The GPC's location is important in terms of associated anatomical structures. It continues in a posterior-superior direction ending at the pterygopalatine fossa communicating with the middle cranial fossa, nasal cavity, and orbit via foramen rotundum, sphenopalatine foramen, and inferior orbital fissure respectively (2).

It goes on in a posterior-superior direction ending at the pterygopalatine fossa and connects with the middle cranial fossa, the nasal cavity, and the orbit via the foramen rotundum, the sphenopalatine foramen, and the inferior orbital fissure respectively (2).

Reaching the pterygopalatine fossa through GPC can be accomplished in maxillary division nerve block in maxillofacial procedures, hemostasis in endoscopic sinus surgery, and relief of sphenopalatine neuralgia (3,4).

The greater and lesser palatine nerves, their posterior inferior lateral nasal branches, and the descending palatine artery are located in this canal (5). Sensory innervation of all maxillary and mandibular teeth and surrounding tissues is provided by the trigeminal nerve.

The maxillary division of the trigeminal nerve (V2) exits the skull through the foramen rotundum and it innervates all maxillary teeth, maxillary palatal and gingival tissue, the nasal cavity, and sinuses (6). The nerve of the pterygoid canal enters the pterygopalatine fossa from the posterior to the foramen rotundum, and transmits the nerve of the pterygoid canal (7). The maxillary nerve receives the sensation of the maxillary teeth, palatal mucosa, and the anatomical structures associated with this region. In major surgical procedures related to the upper jaw, a maxillary nerve block is performed under local anesthesia (8).

The anatomy of these structures undoubtedly affects the anatomy of the GPC due to their proximal relationships. Knowing the anatomy of the GPC is essential for dentists, oral maxillofacial surgeons, and otolaryngologists performing procedures in this area (7,9). When performing surgical procedures, preservation of the descending palatine artery and palatine nerves is essential to avoid excessive bleeding and to maintain nerve supply to the maxilla (10).

The present study aimed to evaluate the morphometry of the GPC and the surrounding anatomical structures using computed tomography.

MATERIAL AND METHODS

This study has been approved by the Afyonkarahisar Health Sciences University, Clinical Research Ethics Committee with approval number 2020/446 and dated 02.10.2020, and was conducted following the Declaration of Helsinki Principles.

The current study was carried out in Afyonkarahisar Health Sciences University, Faculty of Medicine, Department of Anatomy. A total of 100 computed tomography (CT) images with no pathology of 35 female and 65 male subjects aged 12-85 years were selected randomly. The CT images of all individuals who were admitted to the Department of Radiology for any reason were evaluated retrospectively. CT images of individuals with nasal pathology that may affect the measurement and

individuals with poor imaging quality were excluded from the study. The study data were divided into three age groups, <20 years, 20-60 years, and >60 years, as adolescent, adult, and elderly, respectively (11-13).

CT scans were performed with an 80-row Multidetector Computed Tomography (MDCT) scanner (Aquilion Prime, Toshiba Medical Systems, Nasu, Japan). The CT protocol was as follows: peak kilovoltage 120 kVp, tube current, 150-165 mAs; maximum collimation, 2.5 mm; slice thickness, 3 mm; and rotation time, 0.75 s. Images that included the GPC were analyzed retrospectively on a workstation (Aquarius, TeraRecon Inc., San Mateo, CA, USA). Reconstruction images of 0.5 mm slice thickness were created from the 3 mm slice thickness server images. Multiplanar reconstruction and 3D volume rendering (VR) images were obtained from 0.5 mm slice thickness sections. The anatomical landmarks were measured bilaterally on the sagittal and coronal plane (200 sides of 100 cases): a) the beginning diameter, b) the diameter from the widest part, c) the ends diameter, and d) the length of the GPC (Figure 1), e) the entry and f) exit angles of the GPC (Figure 2), g) localization of the GPC entrance with respect to the third molar tooth (distance between the GPC entrance and tooth border), and h) the distance between the GPC entrance and the palatine suture (Figure 3).

Statistical Analysis

All data were analyzed by using IBM SPSS Statistics for Windows, version 19.0 (Armonk, NY: IBM Corp). Descriptive statistics included mean, standard deviation, median, interquartile range, minimum, and maximum values. The Kolmogorov-Smirnov test was used to evaluate the suitability of the data for normal distribution. The differences among the age groups were analyzed with the Kruskal-Wallis test. Mann-Whitney U test was used in comparing the difference between the genders, and sides. The results were evaluated in the 95% confidence interval and $p < 0.05$ were considered statistically significant.

RESULTS

In this study, eight anatomical landmarks related to GPC were measured bilaterally in CT images with no pathology of 100 individuals (35 female, 65 male) with an age range of 12-85 years. Individuals were divided into three groups according to their age; adolescent, adult, and elderly. While the first group consists of 15 people between the ages of 12-20 years, the second group consists of 56 people between the ages of 21-60 years, and the third group consists of 29 people over the age of 60 years.

Regardless of right or left, the mean lengths of GPC was 15.19 ± 4.38 mm. No significant difference was found in any measurements in terms of both gender (Table 1) and sides (Table 2). It has been observed that the diameter measurement from the widest part of the GPC, the distance between the GPC entrance and the palatine suture, and the ends diameter of the GPC increases with age (Table 3).

DISCUSSION

A full understanding of the exact location of the GPC and GPF is required to properly administer anesthesia through this foramen in maxillofacial and related applications. Using GPF as a route for injection has many advantages in local anesthesia for surgeons. Anesthesia is applied in the

hard palate area by inserting a needle into the GPC through the GPF. Thus, the anesthetic solution reaches the pterygopalatine fossa where the maxillary nerve trunk is located. Neurovascular structures within the palatine canal may be at risk also during endoscopic surgery. Possible damage to this area may cause significant blood loss and anesthesia in the ipsilateral hard palate (14). Considering the substantial importance of the exact location of the GPC, this study aimed to determine the length, angle, and diameter of the GPC (2-4,15).

A total of 200 sides of 100 GPC morphologies were evaluated. The diameter of the GPC entrance was found statistically significantly larger in males than females in the young group. GPC length was found statistically significantly greater in females than males in the young group. It has been observed that the diameter measurement from the widest part of the GPC, the distance between the GPC entrance and the palatine suture, and the ends diameter of the GPC increase with age.

The length and angle of the GPC have been determined by using dry skulls, CT, and Conical Beam Computed Tomography (CBCT) studies for different populations.

The length of the GPC of 500 patients had been examined in sagittal sections. In this study, the pterygoid canal was selected as a superior limit of the GPC, and the mean length of the GPC was recorded to be 29 ± 3 mm, ranging from 22 to 40 mm (7).

Sheikhi et al. (16) investigated the length of the GPC of 138 patients in sagittal sections and the mean length was found as 31.8 mm. There was no significant difference between age groups. Ozdede et al. (17) investigated the angle of GPC in different sections. The mean angles of the GPC were determined 156° and 169° in sagittal and coronal sections, respectively. Urbano et al. (18) examined the length of GPC with a dry skull and it was found that 36.40 mm in the female skull and 35.30 mm in the male skull. Tomaszewska et al. (1) conducted a study which is on 150 dry human skulls and 1200 archived adult head CT scans. The length of the right GPC was 29.60 ± 2.50 mm and 32.60 ± 2.80 mm; the left GPC was 29.90 ± 2.70 mm and 32.40 ± 2.80 mm in female and male, respectively. Hwang et al. (19) evaluated the CT scans of 50 patients retrospectively and the mean length of GPC was found 13.80 ± 2.00 mm. Douglas and Wormald (3) investigated GPC length with CT of 22 cadaver heads, and the length of GPC was found 18.50 mm in female individuals. Bahşi et al. (20) examined the length of the GPF-CP with CBCT. The length of the right GPF-CP was 27.48 ± 3.10 mm and 29.27 ± 3.59 mm whereas the length of the left GPF-CP was 26.71 ± 2.82 mm and 29.33 ± 3.14 mm in females and males, respectively. In a CT study evaluating the relationship between facial types and GPC, Lacerda-Santos et al. (21) found that the distance between GPF and the palatine suture was 14.47 ± 1.63 mm on the right and 15.16 ± 1.67 mm on the left and this difference was significant, unlike this study. Ortug and Uzel (22) found the same distance of 14.64 ± 2.20 mm on the right and 14.74 ± 2.22 mm on the left in their measurements on 97 dry skulls and stated that this difference was not significant. Radošević et al. (23) measured the same distance on 174 bone plates and found no difference between right and left, but a difference between males and females.

Different results could have arisen from radiological methods, ethnic origin, the choice's superior limit of GPC, age groups, and genders. We think that the major differences between some studies were due to differences in measurement methodology.

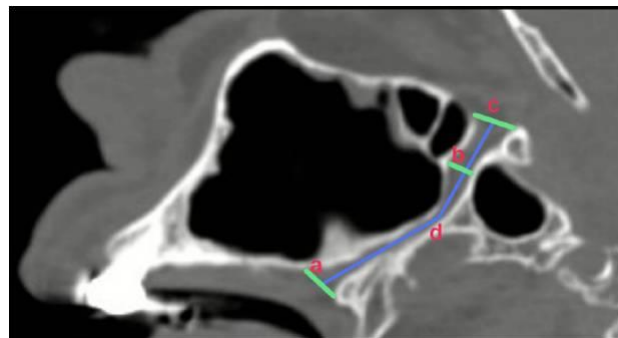


Figure 1. Measurements of the greater palatine canal (GPC) on the sagittal plane, the beginning diameter (a), the diameter measurement from the widest part (b), the ends diameter (c), and the length (d) of the GPC

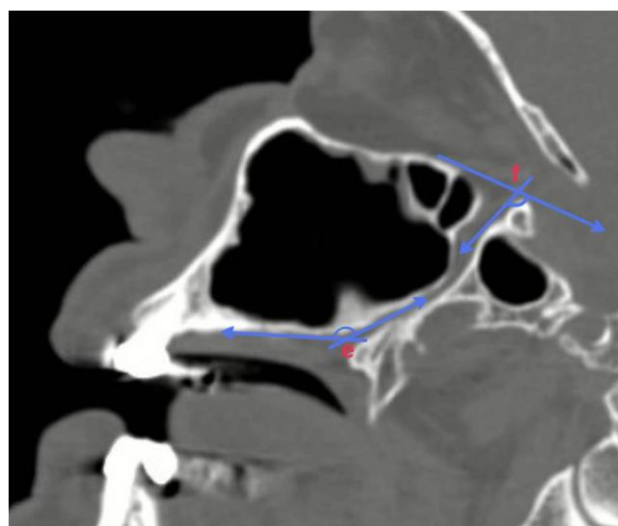


Figure 2. The entry (e) and exit (f) angles of the greater palatine canal (GPC) on the sagittal plane

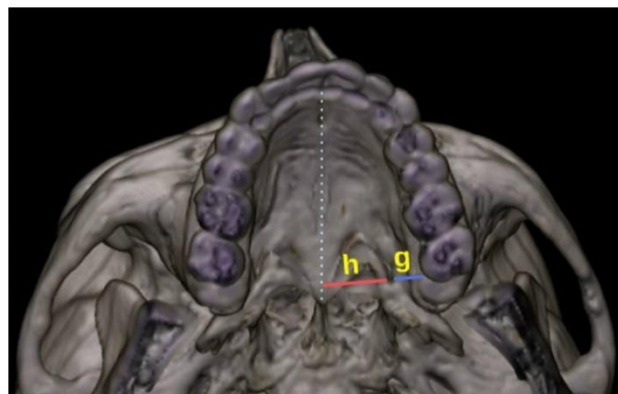


Figure 3. Localization of the greater palatine canal (GPC) entrance, the distance between the GPC entrance and third molar tooth border (g), and palatine suture (h)

Table 1. Comparison between the male and female on the basis of all parameters (all measurements were given in mm)

	Female (n=35)			Male (n=65)			P
	Mean±SD	Median (IQR) [min-max]	Mean±SD	Median (IQR) [min-max]	Mean±SD	Median (IQR) [min-max]	
Diameter of the GPC	4.67±2.15	4.20 (3.07-6.31) [1.14-11.20]	4.99±2.02	4.54 (3.75-5.84) [1.12-11.80]			0.132
Beginning diameter of the GPC	2.55±1.18	2.47 (1.82-3.04) [1.02-6.68]	2.87±1.42	2.56 (2.02-3.36) [0.45-12.20]			0.906
Ends diameter of the GPC	2.48±1.02	2.62 (1.90-2.89) [0.82-5.13]	2.84±1.57	2.77 (1.89-3.42) [0.07-10.80]			0.134
Length of the GPC	15.53±4.04	16.67 (14.67-17.75) [2.72-22.60]	15.00±4.55	15.70 (12.52-17.75) [1.92-25.60]			0.259
Distance between the GPC entrance and tooth border	4.41±1.12	4.35 (3.54-4.95) [2.61-8.39]	4.64±1.56	4.40 (3.62-5.32) [1.73-9.86]			0.647
Distance between the GPC entrance and palatine suture	12.47±2.93	13.35 (11.58-14.22) [3.10-16.40]	13.24±2.20	13.50 (12.05-14.72) [6.50-17.30]			0.144

GPC: greater palatine canal, SD: standard deviation, IQR: interquartile range (25th-75th percentiles)

Table 2. Comparison between the left and right sides on the basis of all parameters (all measurements were given in mm)

	Left (n=100)			Right (n=100)			P
	Mean±SD	Median (IQR) [min-max]	Mean±SD	Median (IQR) [min-max]	Mean±SD	Median (IQR) [min-max]	
Diameter of the GPC	4.90±1.97	4.31 (3.56-5.75) [1.14-11.20]	4.85±2.17	4.48 (3.25-5.57) [1.12-11.80]			0.976
Beginning diameter of the GPC	2.64±1.12	2.48 (1.78-3.33) [0.65-5.73]	2.87±1.54	2.61 (1.84-3.52) [0.45-12.20]			0.302
Ends diameter of the GPC	2.81±1.60	2.60 (1.75-3.58) [0.54-10.80]	2.61±1.18	2.53 (1.69-3.23) [0.07-8.03]			0.519
Length of the GPC	15.16±4.29	15.70 (13.20-17.65) [1.92-25.60]	15.22±4.47	16.20 (13.10-17.95) [2.73-25.00]			0.823
Distance between the GPC entrance and tooth border	4.47±1.34	4.28 (3.48-5.28) [1.98-9.51]	4.64±1.49	4.37 (3.66-5.34) [1.73-9.86]			0.177
Distance between the GPC entrance and palatine suture	12.90±2.43	13.30 (11.85-14.70) [4.20-17.00]	13.03±2.59	13.50 (11.60-14.75) [3.10-17.30]			0.356

GPC: greater palatine canal, SD: standard deviation, IQR: interquartile range (25th-75th percentiles)

Table 3. Comparison of all parameters according to age groups (all measurements are given in mm)

	Group 1 (12-20 years, n=15)			Group 2 (21-60 years, n=56)			Group 3 (60+ years, n=29)			P
	Mean±SD	Median (IQR) [min-max]	Mean±SD	Median (IQR) [min-max]	Mean±SD	Median (IQR) [min-max]	Mean±SD	Median (IQR) [min-max]		
Diameter of the GPC	4.61±1.73	4.35 (2.91-6.02) [1.12-7.19]	4.53±1.93	4.16 (3.40-5.64) [1.75-9.05]	5.68±2.30	5.34 (3.97-6.89) [2.68-11.80]				0.713
Beginning diameter of the GPC	2.92±1.39	3.01 (1.53-4.02) [0.45-5.05]	2.61±1.41	2.39 (1.98-3.00) [1.11-7.79]	2.94±1.18	3.01 (2.18-3.85) [1.51-12.20]				0.416
Ends diameter of the GPC	2.28±0.93	1.99 (1.68-3.01) [0.07-3.10]	2.56±1.29	2.65 (1.89-3.08) [1.04-6.35]	3.22±1.69	3.01 (2.34-4.08) [1.35-10.80]				0.650
Length of the GPC	15.23±3.61	16.75 (13.10-17.60) [1.92-20.10]	15.27±4.59	15.45 (13.30-18.05) [5.13-25.10]	15.01±4.35	16.90 (12.55-17.75) [4.08-25.60]				0.783
Distance between the GPC entrance and tooth border	4.48±1.04	4.45 (3.46-4.94) [1.73-6.44]	4.69±1.46	4.65 (3.76-5.30) [2.73-9.15]	4.34±1.50	4.14 (3.38-5.21) [2.33-9.86]				0.508
Distance between the GPC entrance and palatine suture	11.28±3.13	11.95 (9.36-13.90) [3.10-13.10]	12.94±2.47	13.20 (11.60-14.65) [4.68-17.05]	13.89±1.65	13.95 (12.90-14.75) [9.73-17.30]				0.554

GPC: greater palatine canal, SD: standard deviation, IQR: interquartile range (25th-75th percentiles)

The limitation of our study can be considered as the small number of cases. Therefore, the number of subjects in the groups is not homogeneous.

CONCLUSION

Given all the distances measured, this study could help clinicians to more precisely localize the GPC in patients and predict to numb the maxillary nerve with low complication. It can be concluded that further CT-based studies are needed to estimate the length and other related measurements of the GPC in different ethnic groups.

Ethics Committee Approval: The study was approved by the Clinical Research Ethics Committee of Afyonkarahisar Health Sciences University (02.10.2020, 446).

Conflict of Interest: None declared by the authors.

Financial Disclosure: None declared by the authors.

Acknowledgments: None declared by the authors.

Author Contributions: Idea/Concept: HG, OT; Design: HG, OT; Data Collection/Processing: EH, ÇÖG; Analysis/ Interpretation: HG, EK, ÇÖG; Literature Review: HG, EK; Drafting/Writing: HG, EH; Critical Review: OT, EH.

REFERENCES

1. Tomaszewska IM, Tomaszewski KA, Kmiołek EK, Pena IZ, Urbanik A, Nowakowski M, et al. Anatomical landmarks for the localization of the greater palatine foramen--a study of 1200 head CTs, 150 dry skulls, systematic review of literature and meta-analysis. *J Anat.* 2014;225(4):419-35.
2. Erdogan N, Unur E, Baykara M. CT anatomy of pterygopalatine fossa and its communications: A pictorial review. *Comput Med Imaging Graph.* 2003;27(6):481-7.
3. Douglas R, Wormald PJ. Pterygopalatine fossa infiltration through the greater palatine foramen: Where to bend the needle. *Laryngoscope.* 2006;116(7):1255-7.
4. McKinney KA, Stadler ME, Wong YT, Shah RN, Rose AS, Zdanski CJ, et al. Transpalatal greater palatine canal injection: Radioanatomic analysis of where to bend the needle for pediatric sinus surgery. *Am J Rhinol Allergy.* 2010;24(5):385-8.
5. Apenhasmit W, Chompoopong S, Methathrathip D, Sangvichien S, Karuwanarint S. Clinical anatomy of the posterior maxilla pertaining to Le Fort I osteotomy in Thais. *Clin Anat.* 2005;18(5):323-9.
6. Norton NS. *Netter's head and neck anatomy for dentistry*, 2nd ed. Philadelphia: Elsevier; 2012.
7. Howard-Swirzinski K, Edwards PC, Saini TS, Norton NS. Length and geometric patterns of the greater palatine canal observed in cone beam computed tomography. *Int J Dent.* 2010;2010:292753.
8. Narayan RK, Ghosh SK. Can the morphological attributes of greater palatine foramen have implications in maxillary nerve block? An analytical study using anatomical planes. *Transl Res Anat.* 2021;22:100093.
9. Lepere AJ. Maxillary nerve block via the greater palatine canal: new look at an old technique. *Anesth Pain Control Dent.* 1993;2(4):195-7.
10. White SC, Pharoah MJ. *Oral radiology. Principle and interpretation*, 7th ed. Missouri: Elsevier; 2013.
11. Horng WB, Lee CP, Chen CW. Classification of age groups based on facial features. *J Appl Sci Eng.* 2001;4(3):183-91.
12. Mehra A, Karjodkar FR, Sansare K, Kapoor R, Tambawala S, Saxena VS. Assessment of the dimensions of the pterygoid hamulus for establishing age- and sex-specific reference standards using cone-beam computed tomography. *Imaging Sci Dent.* 2021;51(1):49-54.
13. Abdullah WH, Abbas Alhussaini AH. The role of cone beam computed tomography in determination of the greater palatine foramen position among Iraqi population. *J Bagh Coll Dent.* 2018;30(1):53-7.
14. Campbell RG, Solares CA, Mason EC, Prevedello DM, Carrau RL. Endoscopic endonasal landmarks to the greater palatine canal. A radiographic study. *J Neurol Surg B Skull Base.* 2018;79(4):325-9.
15. Tomaszewska IM, Kmiołek EK, Pena IZ, Średniawa M, Czyżowska K, Chrzan R, et al. Computed tomography morphometric analysis of the greater palatine canal: a study of 1,500 head CT scans and a systematic review of literature. *Anat Sci Int.* 2015;90(84):287-97.
16. Sheikhi M, Ghorbanizadeh S, Abdinian M, Goroochi H, Badrian H. Accuracy of linear measurements of galileos cone beam computed tomography in normal and different head positions. *Int J Dent.* 2012;2012:214954.
17. Özdede M, Keriş Yıldız E, Altunkaynak B, Peker İ. Morphometric analysis of greater palatine canal via cone-beam computed tomography. *Balk J Dent Med.* 2018;22(3):150-6.
18. Urbano ES, Melo KA, Costa ST. Morphologic study of the greater palatine canal. *J Morphol Sci.* 2010;27(2):102-4.
19. Hwang SH, Seo JH, Joo YH, Kim BG, Cho JH, Kang JM. An anatomic study using three-dimensional reconstruction for pterygopalatine fossa infiltration via the greater palatine canal. *Clin Anat.* 2011;24(5):576-82.
20. Bahşi İ, Orhan M, Kervancıoğlu P, Yalçın ED. Morphometric evaluation and clinical implications of the greater palatine foramen, greater palatine canal and pterygopalatine fossa on CBCT images and review of literature. *Surg Radiol Anat.* 2019;41(5):551-67.
21. Lacerda-Santos JT, Granja GL, de Freitas GB, Manhães Jr LRC, de Melo DP, Dos Santos JA. The influence of facial types on the morphology and location of the greater palatine foramen: a CBCT study. *Oral Radiol.* 2022;38(3):337-43.
22. Ortug A, Uzel M. Greater palatine foramen: assessment with palatal index, shape, number and gender. *Folia Morphol (Warsz).* 2019;78(2):371-7.
23. Radošević D, Erić M, Marić D, Vučinić N, Knezi N, Pupovac N, et al. Morphology of the greater palatine foramen: a clinical point of view. *Surg Radiol Anat.* 2023;45(8):1001-7.